Acta Geodyn. Geomater., Vol. 18, No. 1 (201), 91–101, 2021
DOI: 10.13168/AGG.2021.0007
journal homepage: https://www.irsm.cas.cz/acta

ORIGINAL PAPER

BRITTLENESS INDEX OF COAL FROM THE UPPER SILESIAN COAL BASIN

Rafał MOSKA

Oil and Gas Institute - National Research Institute, Lubicz 25 A, 31-503 Krakow, Poland

**Corresponding author's e-mail:* moska@inig.pl

ARTICLE INFO

Article history:
Received 4 October 2020
Accepted 15 February 2021
Available online 3 March 2021

Keywords:
Brittleness index
Rock mechanics
Ultrasonic laboratory measurements
Dynamic elastic parameters
Coal
Maceral composition

ABSTRACT

A growing interest in the field of coal bed methane (CBM) extraction in Poland shows the demand for rock mechanics data, used to design hydraulic fracturing operations. The elastic response of the rock is typically determined by sonic logging calibrated with laboratory tests. This paper presents the laboratory ultrasonic measurements of the core samples, performed to determine the elastic moduli and brittleness index (*BI*) of the coal. Tests were performed on 20 core plugs from four coal mines located in the central and southern part of the Upper Silesian Coal Basin (USCB), Poland, characterized by varied maceral composition and mineral additives. The samples were cored out in three directions: perpendicular, parallel, and at a 45° angle to the bedding planes, and tested with the given effective pressure. The majority of the samples were saturated by water with a potassium chloride additive (swelling inhibitor). A P- and S-wave velocity upward trend was observed when the mineral content in the samples increased. Elevated velocities in samples of high mineral content resulted in exceeding the E_d to v_d limits for coal as proposed in literature. With increased *BI*, upward trends in the liptinite and inertinite content as well as a downward trend in the vitrinite content were observed. The dynamic elastic moduli of the measured samples were compared to the available literature data.

1. INTRODUCTION

The need for diversification of the natural gas resources in Poland has resulted in a growing interest in unconventional deposits, including coal bed methane (CBM). The documented balance of CBM resources in the Upper Silesian Coal Basin (USCB), according to experts from the Polish Geological Institute – National Research Institute, amount to 102 billion m^3 of natural gas (Malon and Tymiński, 2019). The production of this gas from unconventional reservoirs is much more complicated than from conventional ones. Coal matter includes methane in the following forms: adsorbed in micropores of diameter less than 2 mm, in a carbon matrix, bound by weak van der Waals's bonds on the carbon surface, such as free gas in cracks and natural fractures or dissolved in water (Gonet et al., 2010).

To release the gas, hydraulic fracturing is required in the low permeability productive horizon, similarly to shale gas deposits (Kasza, 2019). In recent years, a few hydraulic fracturing operations were created as directional and horizontal boreholes on the Gilowice deposit (the southern part of USCB). The determination of the elastic parameters of the reservoir and surrounding formations are one of the keys to effective fracking. The elastic moduli of the rock, together with the pore pressure and stress state in the reservoir, determines the length and width of the inducted fractures. Rock mechanics data can be obtained from acoustic well logging or from laboratory tests (dynamic and static). The laboratory measurements of the dynamic Young's modulus (E_d) and Poisson's ratio (v_d) of the different rocks have been conducted for many years; however, only a small part of the work was based on coal material.

The concept of the brittleness index (*BI*) was developed in the 1960s, in response to the demand for a parameter describing a part of the elastic properties of the rock related to the deformation characteristics. Throughout the years, many authors used various geological and geophysical parameters to calculate *BI* based on the:

- shape of stress-strain curve (Bishop, 1967; Hucka and Das, 1974; Hajiabdolmajid and Kaiser, 2003),
- energy balance analysis (Tarasov and Potvin, 2013),
- unconfined compressive strength and Brazilian tensile strength tests (Hucka and Das, 1974; Altindag, 2002),
- mineral composition (Jarvie et al., 2007; Wang and Gale, 2009; Jin et al., 2014a; Jin et al., 2014b; Bała, 2017),
- Young's modulus to Poisson's ratio relation (Grieser and Bray, 2007; Rickman et al., 2008; Luan et al., 2014; Bała, 2017; Moska et al., 2018; Wu et al., 2019),

- combined mineralogy-based and elastic parameters-based methods (Qian et al., 2020).

Regardless of the method of *BI* definition, brittle rocks typically exhibit a unique set of features (Zhang et al., 2016):

– low elongation upon load application,
– higher ratio of compressive strength to tensile strength,
– higher internal friction angles (high friction angled brittle rocks have less possibility to slip along the fracture,
– greater percentage of brittle minerals (e.g., quartz) and minimal amounts of ductile minerals (e.g., clay minerals),
– higher *E* and lower *v* values, where these terms describe the rock's ability to fail and maintain inducted fractures, respectively.

The set of rock characteristics mentioned above is very desirable in the oil and gas industry, due to the susceptibility to brittle crack development during hydraulic fracturing. *BI* not only reflects the deformation characteristics directly but also indirectly determines the type of the fracking fluid and proppant.

Fluid pumped above the breakdown pressure causes a burst in a rock and create an inducted fracture, perpendicular to the minimum stress direction. Young's modulus defines how much energy is required to accomplish rock displacement during fracture formation. Brittle rocks with large *E* require more of energy. In these formations fractures tend to be relatively narrow and long, whereas in ductile rocks of low *E*, short fractures of relatively large width dominate (Economides and Martin, 2007).

Pressure drops below the closure pressure cause tightening of the fracture, which is counteracted by grains of proppant transported with fracking fluid. Due to the low plastic deformations in brittle rocks, the embedment phenomena are reduced, and thus conductivity through propped fractures is preserved for a longer time (Alramachi and Sundberg, 2012; Masłowski et al., 2019).

The high length and low width of the fractures in brittle formations require low viscosity fluids to reduce a flow resistance. Due to the low permeability of such rocks, the fracking fluid should cause slight conductivity damage (Czupski et al., 2013).

In the oil and gas industry, predominantly the *E* to *v* ratio defines the *BI*. The *BI* profile, based on well logging data, is determined along the reservoir production zone. These data are often calibrated by laboratory tests on core plugs. On this basis, the sweet spots with optimal *BI* are marked as indicators for perforation. (Grieser and Bray, 2007).

Laboratory ultrasonic measurements of coal samples have not been widely disseminated so far. This situation changed in recent years due to the growing interest in CBM extraction. The described results of the ultrasonic measurements of coal concerned the relationship between the elastic moduli and confining pressure and water saturation (Yu et al., 1993), petrographic parameters and coal rank (Garcia-Gonzalez and Towle, 2006; Morcote et al., 2010; Kumar et al., 2015), as well as anisotropy and *BI* (Wu et al., 2015; Wu et al., 2019). Wu et al. (2019), in response to the lack of clear criteria for the evaluation of *BI* for coal samples, suggested constant limit values for the E_d and v_d moduli, allowing the strength of samples to be described connected with the coal structure (coal type, fractures, and bedding).

Data concerning the rock mechanics ultrasonic measurements of the coal samples from USCB are unavailable in the literature so far. A first attempt at ultrasonic tests of coal from USCB were shown in 2019; however, that paper included the data of single samples and was an attempt to gather experience in sample preparation and test conduction (Moska and Masłowski, 2019). Still, a growing interest in CBM extraction in Poland shows demand for these kinds of data, and allows for the continuance of those studies.

In this paper, 20 coal samples of known maceral composition, from four coal mines, were tested. The obtained dynamic elastic moduli were used for the *BI* calculations, based on the criteria from (Wu et al., 2019). Finally, an attempt to relate the rock mechanics properties to the maceral composition was conducted.

2. MATERIALS AND METHODS

2.1. MATERIALS

Blocks of coal were collected from four coal mines (A, B, C, and D were the sample IDs) located in the central and southern part of USCB and transported to the laboratory in sealed containers. Samples from the D coal mine were collected from several excavations (D1, D2, D3, and D5 were the sample IDs). A total of 20 core samples were cut out, using a construction core driller, in three directions: perpendicular, parallel, and at an angle of 45° to the bedding planes, according to the methodology of Vernik (1993) ($_V$, $_H$, and $_{45}$ were the sample IDs, respectively). Samples 1–8 were 1 inch in diameter, whereas samples 9–20 were 1.5 inch. The length of the samples amounted to from 34 to 40 mm and from 40 to 60 mm, respectively for the two groups. The top and bottom faces were planed up to gain a smooth surface and perpendicularity (Figs. 1, 2).

First, the effective porosity and bulk density measurements were conducted using an HPG-100 helium porosimeter. The development of natural unfilled fractures and the crack network in samples was specified by macroscopic observations. Samples 4 to 20 were saturated by water with 2 % potassium chloride (KCl, swelling inhibitor) by a minimum of 12 hours in a vacuum chamber, at the underpressure of 1 Bar. Table 1 presents a list of the measured samples, descriptions, and selected parameters.

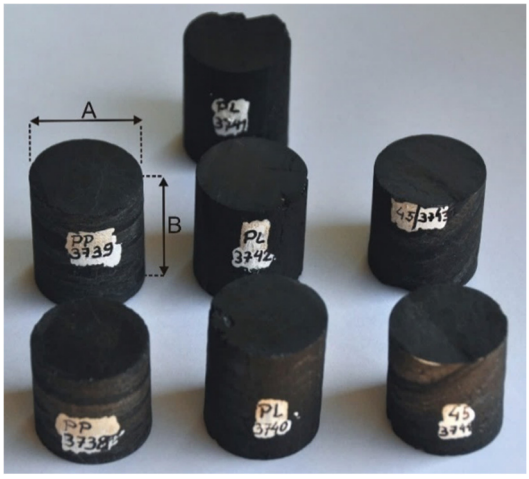

Fig. 1 Coal samples from the A and B coal mines before testing. Dimensions: A—1 in. and B—about 35–40 mm depending on the sample.

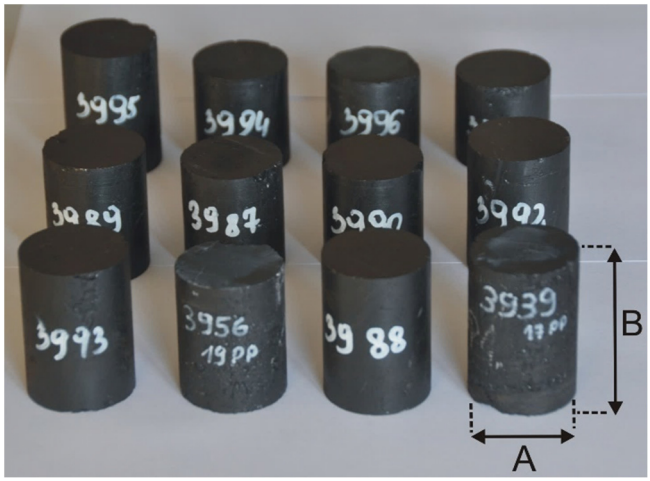

Fig. 2 Coal samples from the C and D coal mines before testing. Dimensions: A—1,5 in. and B—about 40–60 mm depending on the sample.

Table 1 Selected parameters of measured samples.

Sample ID	Porosity (%)	Unfilled fractures and cracks	Lithotype. After: Diessel (1965) and Diessel (1992)
$1A_V$	2.71	undeveloped	Banded dull coal
$2A_H$		moderate	Banded dull coal
$3A_{45}$		moderate	Banded dull coal
$4B_V$	2.74	undeveloped	Banded coal
$5B_V$	2.73	undeveloped	Banded coal
$6B_H$		moderate	Banded bright coal
$7B_H$	2.15	moderate	Banded bright coal
$8B_H$	2.70	undeveloped	Banded bright coal
$9C_V$	5.20	developed	Banded dull coal
$10C_V$	7.22	developed	Banded dull coal
$11D1_H$	3.19	moderate	Banded bright coal
$12D2_H$	2.33	undeveloped	Banded coal
$13D2_H$	2.85	undeveloped	Banded coal
$14D2_H$	2.88	moderate	Banded coal
$15D3_H$	4.07	undeveloped	Banded dull coal
$16D5_H$	3.14	undeveloped	Banded coal
$17D5_H$	3.03	undeveloped	Banded coal
$18D5_H$	3.18	moderate	Banded coal
$19D5_H$	4.10	moderate	Banded coal
$20D5_V$	6.15	undeveloped	Banded coal

2.2. METHODS

The maceral composition analysis was conducted on polished specimens, using an optical microscope Zeiss Imager M2. First, the surface of the specimens was observed in reflected and UV light, to identify fragments of organic matter. Secondly, the planimetric analysis of about 500 points at the surface were performed, which allows us to obtain proportions between macerals. The analysis was based on the classification and terminology given by International Committee for Coal and Organic Petrology (ICCP) (ICCP, 1998; ICCP, 2001; Sykorova et al., 2005; Pickel et al., 2017). The lithotypes of the samples were classified based on the ratio of vitrinite to other maceral contents (Diessel, 1965; Diessel, 1992).

Ultrasonic tests were conducted using the Vinci AVS-700 device, under the following conditions: temperature of approximately 25 °C, effective

pressure of 9.72 MPa, which corresponds to the average effective pressure at the depth of collecting the samples. The transition measurement method was used. The transducer frequency was set to 500 MHz, which allowed a good-quality signal for 1 to 3" length samples. For each of the samples, the P-wave velocity and two S-waves perpendicular to each other were measured. The velocity of the S-wave was calculated as an arithmetic average of both S-waves. Examples of the measured waveforms are presented in Figure 3.

he elastic moduli of the samples were calculated using the equations below:

$$v_d = \frac{\frac{1}{2}-\left(\frac{V_S}{V_P}\right)^2}{1-\left(\frac{V_S}{V_P}\right)} \quad (1)$$

$$E_d = \rho \frac{V_P^2(1+v_d)(1-v_d)}{(1-v_d)} \quad (2)$$

$$G_d = \rho V_S^2 \quad (3)$$

$$K_d = \rho V_P^2 - \frac{3}{4} V_S^2 \quad (4)$$

where V_P and V_S are the compressive and shear waves velocity, respectively; ρ is the bulk density of the sample; and v_d, E_d G_d, and K_d are the Poisson's, Young's, shear, and bulk elastic moduli, respectively.

The *BI* was calculated based on Rickman's et al. (2008) methodology using the relation between the dynamic Young's modulus and dynamic Poisson's ratio.

$$BI = \frac{\left[\frac{100(E_d - E_{d\,\min})}{(E_{d\,max} - E_{d\,\min})} + \frac{100(v_d - v_{d\,\max})}{(v_{d\,min} - v_{d\,\max})}\right]}{2} \quad (5)$$

where E_d and v_d are the measured Young's modulus and Poisson's ratio, respectively; $E_{d\,min}$ and $E_{d\,max}$ are the minimum and maximum Young's moduli; and $v_{d\,min}$ and $v_{d\,max}$ are the minimum and maximum Poisson's ratios, respectively. To unify the calculation standard, I assumed the limit values of E_d and v_d after Wu et al., (2019), and set $E_{d\,min}$ and $E_{d\,max}$ as 0.5–9.0 GPa, and $v_{d\,min}$ and $v_{d\,max}$ as 0.22–0.45 (-).

3. RESULTS

Results of the maceral composition analysis as well as ultrasonic tests of the samples are presented in Tables 2, 3 and Figure 4.

4. DISCUSSION

4.1. MACERAL COMPOSITION

Based on the results from Table 2, the tested samples can be divided into four groups. In the first group (I), the banded dull coal samples $1A_V$–$3A_{45}$, contained significant amounts of liptinite and inertinite macerals (36 % and 45 %, respectively), the vitrinite content was slightly lower (19 %), and the mineral content was vestigial. Samples 2 and 3 had fractures unfilled by mineral matter, formed after the sample preparation.

The composition of the second group (II) included banded coal ($4B_V$, $5B_V$) and banded bright coal (and $6B_H$–$8B_H$) were dominated by the vitrinite group (58 %–68 %), whereas liptinite and inertinite were minor. Samples $4B_V$ and $5B_V$ were characterized by a significant increased content of the mineral matter, which filled the microcracks and fractures. The lower amount of minerals caused an increased proportion of liptinite and inertinite in the other samples in this group.

Samples $9C_V$ and $10C_V$ (banded dull coal) were assigned to group III, due to their low vitrinite content (25 %–35 %), relatively little mineral addition, and large amount of macerals from the inertinite group. These two samples were clearly distinguish by the number of unfilled cracks and fragility.

Group IV, mostly banded coal, was represented by samples $11D1_H$ to $20D5_V$ and characterized by variable proportions of vitrinite to inertinite, and a slight content of liptinite (up to 14 %) and minerals (up to 2 %). Macroscopically visible cracks in the structure of these samples were undeveloped or moderately developed. Microscopic images of selected macerals at the surface of the specimens are shown in Figure 4.

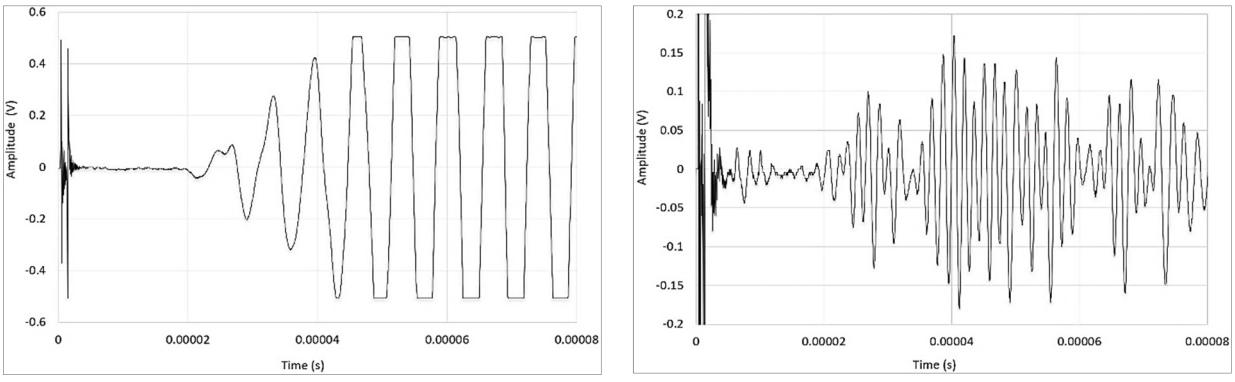

(a) (b)

Fig. 3 Examples of: (a) P-waveform and (b) S-waveform. Data from 9CV sample.

Table 2 The contents of the macerals and mineral additives in the tested coal samples.

No.	Sample ID	Vitrinite (%)	Liptinite (%)	Inertinite (%)	Minerals (%)
1	$1A_V$				
2	$2A_H$	18.89	35.98	45.13	vestigial
3	$3A_{45}$				
4	$4B_V$	58.01	3.25	4.06	34.69
5	$5B_V$	58.51	0.78	2.74	37.96
6	$6B_H$	61.55	11.04	20.45	6.95
7	$7B_H$	62.65	11.22	20.61	5.51
8	$8B_H$	67.56	10.06	12.11	10.27
9	$9C_V$	35.25	8.12	56.44	0.20
10	$10C_V$	25.55	1.21	65.39	7.85
11	$11D1_H$	76.27	5.68	17.44	0.61
12	$12D2_H$	59.34	7.13	33.14	0.39
13	$13D2_H$				
14	$14D2_H$	42.39	13.49	43.55	0.58
15	$15D3_H$	24.66	7.38	66.41	1.55
16	$16D5_H$	49.42	5.64	44.75	0.19
17	$17D5_H$				
18	$18D5_H$	50.10	6.91	42.80	0.19
19	$19D5_H$				
20	$20D5_V$	48.00	5.40	44.60	2.00

Table 3 The wave velocities, dynamic elastic moduli, and BI parameters of the measured coal samples.

No.	Sample ID	Density ρ (g/cm^3)	V_P (m/s)	V_S (m/s)	V_P/V_S (-)	ν_d (-)	E_d (GPa)	G_d (GPa)	K_d (GPa)	BI (%)
Dry samples										
1	$1A_V$	1.28	2378	1261	1.89	0.30	5.32	2.04	4.54	61.69
2	$2A_H$	1.27	2430	1328	1.83	0.29	5.77	2.24	4.51	66.42
3	$3A_{45}$	1.28	2418	1298	1.86	0.30	5.61	2.16	4.62	63.39
Water saturated samples										
4	$4B_V$	1.94	2700	1438	1.88	0.30	10.44	4.01	8.77	91.80
5	$5B_V$	1.95	2824	1650	1.71	0.24	13.18	5.31	8.46	120.42[1]
6	$6B_H$	1.49	2697	1471	1.83	0.29	8.30	3.22	6.54	81.30
7	$7B_H$	1.38	2293	1207	1.90	0.31	5.27	2.01	4.58	59.31
8	$8B_H$	1.50	2989	1700	1.76	0.26	10.92	4.33	7.60	102.96[1]
9	$9C_V$	1.35	1969	1076	1.83	0.29	4.01	1.56	3.14	56.06
10	$10C_V$	1.41	2131	1202	1.77	0.27	5.16	2.04	3.67	67.00
11	$11D1_H$	1.34	2064	1076	1.92	0.31	4.07	1.55	3.63	52.25
12	$12D2_H$	1.31	2040	1118	1.82	0.29	4.20	1.63	3.26	57.18
13	$13D2_H$	1.31	1928	1052	1.83	0.29	3.73	1.45	2.93	54.42
14	$14D2_H$	1.31	2051	1011	2.03	0.34	3.58	1.34	3.72	43.12
15	$15D3_H$	1.39	1883	1022	1.84	0.29	3.74	1.45	2.98	54.48
16	$16D5_H$	1.33	1977	1166	1.71	0.24	4.47	1.80	2.88	69.19
17	$17D5_H$	1.35	2150	1172	1.83	0.29	4.78	1.86	3.77	60.59
18	$18D5_H$	1.31	2269	1065	2.13	0.36	4.08	1.50	4.76	41.89
19	$19D5_H$	1.33	1995	1167	1.71	0.24	4.50	1.81	2.88	69.36
20	$20D5_V$	1.37	2130	990	2.15	0.36	3.66	1.34	3.93	39.42

[1] *BI* over 100 % of the results from the increased content of mineral matter in coal samples.

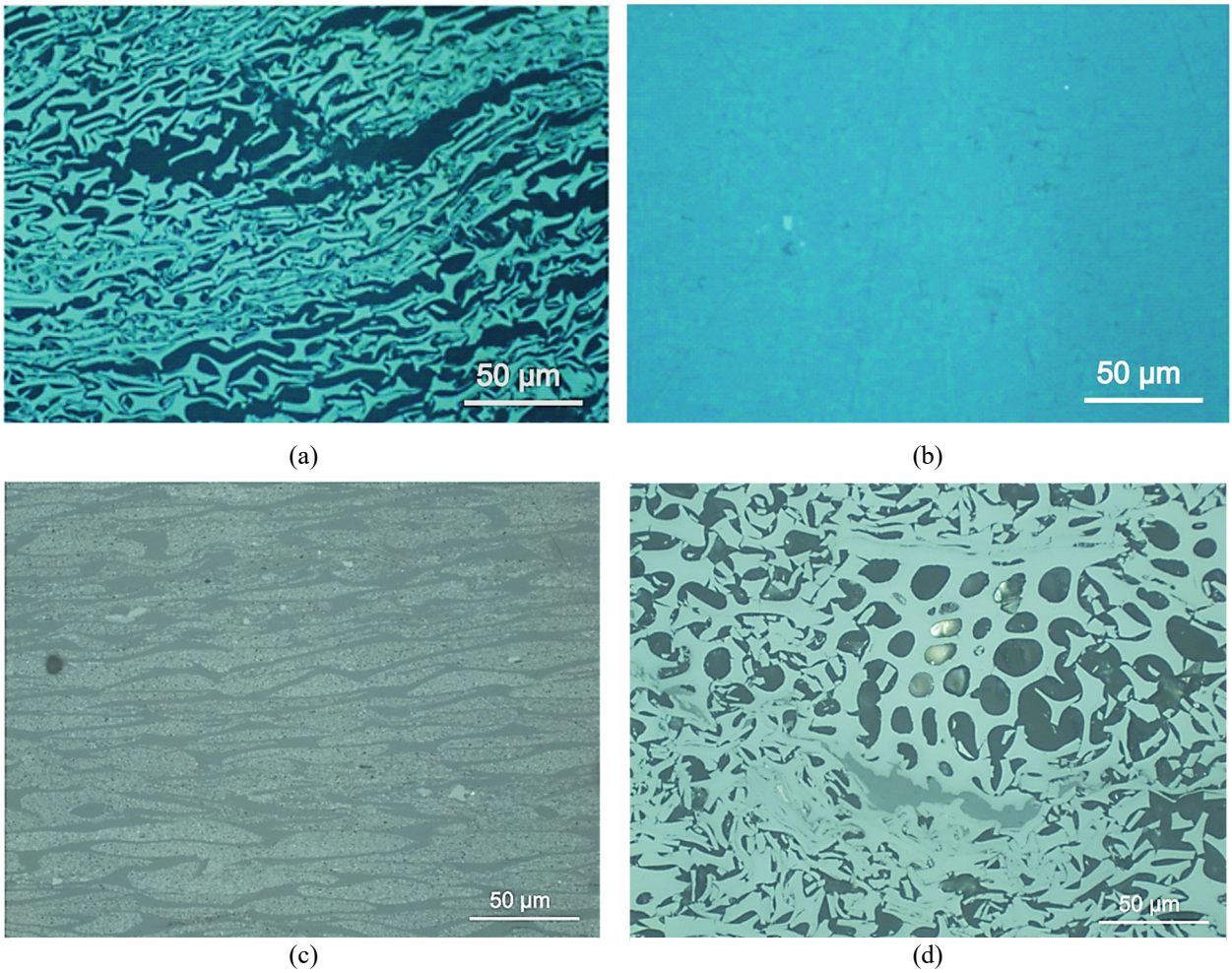

(a) (b)

(c) (d)

Fig. 4 Microscopic images of selected macerals at the surface of the specimens: (a) Fuzinite (inertinite group) in the $1A_V$ sample, reflected light; (b) Kolotelinite (vitrinite group) in the $7B_H$ sample, reflected light; (c) Mikrinite (inertinite group) fillings and the relicts of the cellular structure in the $15D2_H$ sample, reflected light; and (d) Semifuzinite (inertinite group) in the $10C_V$ sample, reflected light.

4.2. DYNAMIC ELASTIC MODULI AND BRITTLENESS

Looking at Table 3, a significant variability of the velocities can be seen. The P-wave velocities in the dry samples $1A_V$–$3A_{45}$, were similar and amounted approximately 2400 m/s. The S-wave velocities were lower by approximately 1100 m/s, which gave a V_P/V_S ratio of 1.83–1.89. Due to the confining pressure (almost 10 MPa), most of cracks were closed; thus, the slight anisotropy in velocities depend mostly on the arrangement of the layers—the highest velocity was in the horizontal sample, and the lowest was in the vertical sample. The dynamic elastic moduli amounted 0.29–0.30 (-) in v_d and 5.32–5.77 GPa in E_d, which resulted in a *BI* in the range of 61.69 %–66.41 %.

Samples $4B_V$–$8B_H$ were characterized by a significantly increased bulk density—caused in part by brine saturation, but primarily due to the high content of mineral additives, which exceeded the average density of bituminous coal available in the literature (Attachment 1). This resulted in elevated P- and S-wave velocities (approximately 2700–2800 and 1450–1650 m/s, respectively) in the $4B_V$ and $5B_V$ samples. The velocities of the waves in the $8B_H$ sample (2900 and 1700 m/s for P- and S-waves, respectively), were caused by the presence of a strongly cementing mineral content and presumably by less-developed unfilled cracks, oriented parallel to the bedding planes. The variability in the maceral mineral content in samples 4–9 did not allow the observation of any influence of the direction of measurement on the velocities. Samples with a lower mineral content ($6B_H$, $7B_H$,) were characterized by E_d below 10 GPa and v_d between 0.29–0.37 (-), which is similar to the typically described coal samples in the literature (Attachment 1).

The remaining B samples showed an elevated E_d modulus with a reduced v_d ratio (above 10 GPa and about 0.25, respectively), which corresponds to the values published for sandstones and shales (e.g., Bała, 1990; Jizba, 1991). Elevated E_d resulted in the *BI* exceeding the limits given by Wu et al. (2019) for the

coal samples, which is shown in Figures 6 and 7. A *BI* above 100% in samples $5B_V$ and $8B_H$ suggests that such a coal-mineral mixture should not be considered as coal, even though coal is the primary component in this rock. On the other hand, the wider-range limit *BI* index given by Grieser and Bray (2007) is unsuitable for coal because it does not reflect the susceptibility fracking of coal due to its pre-existing cracks and fractures. Assuming that the *BI* limits for coal samples given by Wu et al. (2019) are correct, then values exceeding 100 % indicate an elevated content of high stiffness mineral matter in relation to coal, but likely do not reflect a further increasing susceptibility for fracking.

Samples $9C_V$ and $10C_V$, of a lower bulk density than the previous samples, were characterized by velocities in the range of about 2000–2100 m/s for P-waves and about 1200 m/s for S-waves. Despite a developed, pre-existing fracture system, v_d remained below 0.3 (-), which reflects the relatively small deformation perpendicular to the stress direction. Dynamic Young's modulus, amounting to 4.0–5.2 GPa, allowed the calculation of *BI* in the range of 56 %–67 %.

The group of samples from the D coal mine were collected from several locations, and demonstrated various elastic properties. The velocities of the P- waves were in the range from about 1900 to

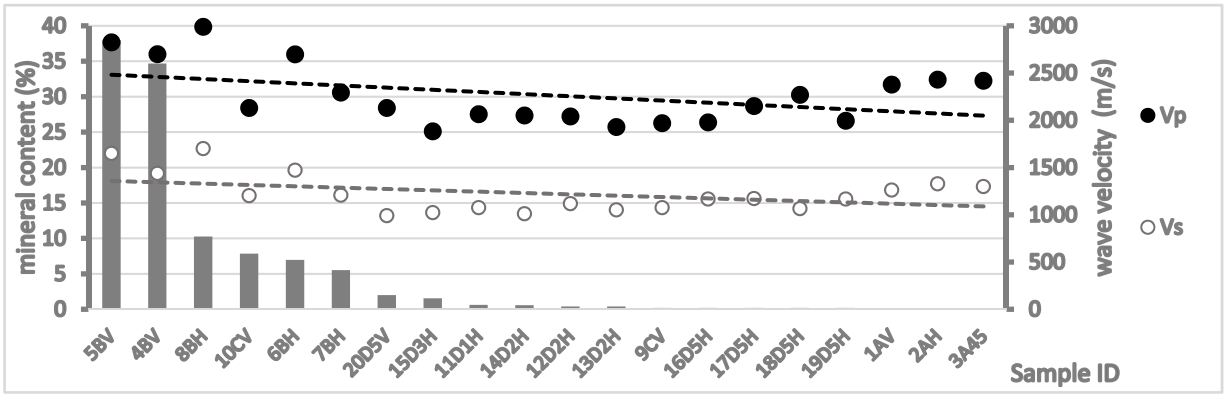

Fig. 5 The relationship between the mineral content and wave velocities in the measured samples. Black dashed line: trend line (V_P), and light grey dashed line: trend line (V_S).

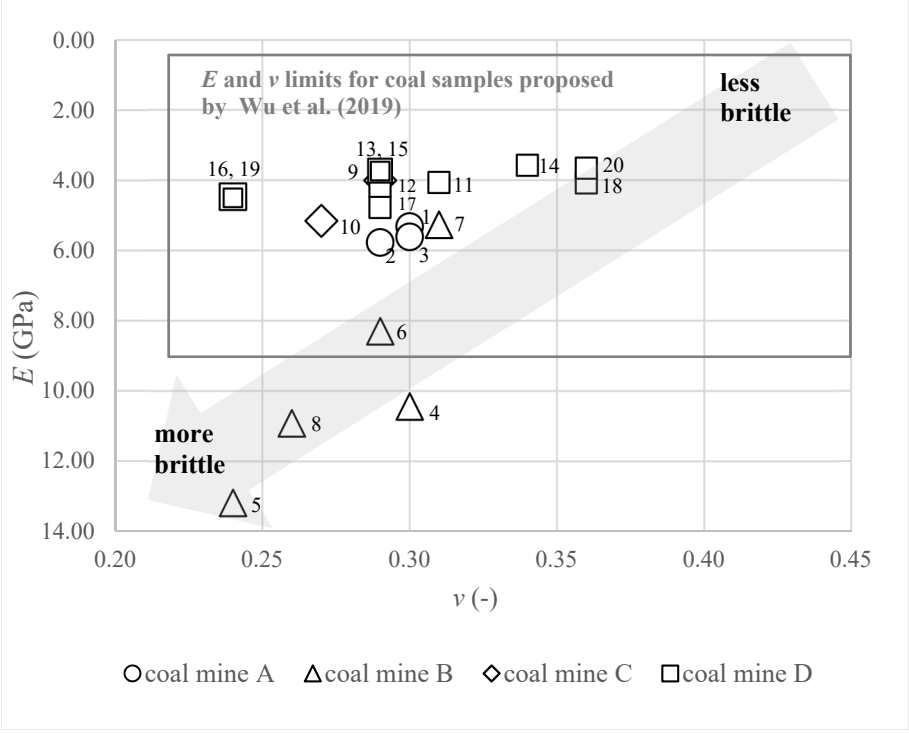

Fig. 6 The dynamic Young's modulus (E_d) vs. the dynamic Poison's ratio (v_d) relation for the measured samples.

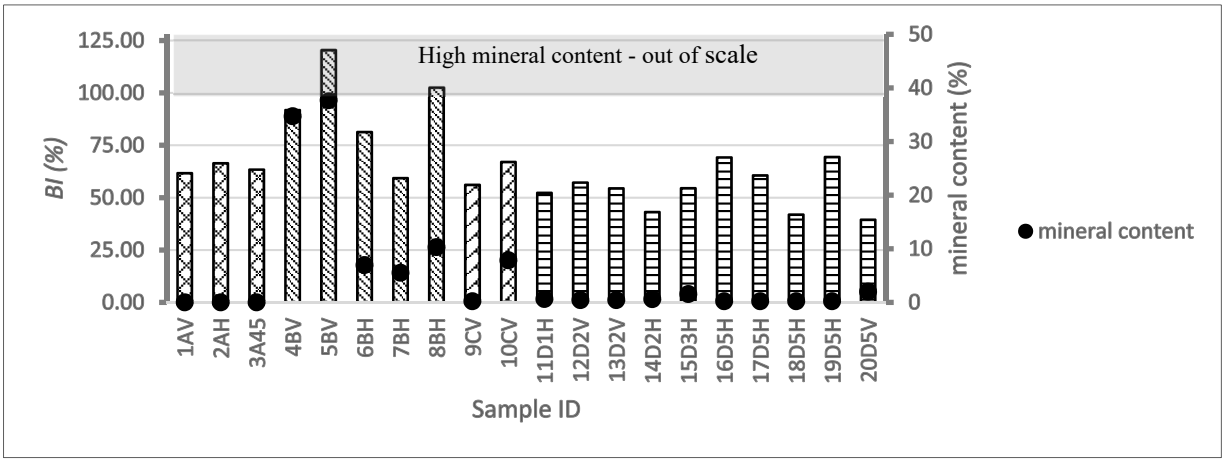

Fig. 7 Relationship between the brittleness and mineral content in the measured coal samples.

2300 m/s whereas S-waves were from 1000 to 1200 m/s. This resulted in a wide range of V_P/V_S ratios (1.71–2.15), ν (0.24–0.36), and a slightly higher E_d, compared to the samples from other coal mines. Interestingly, the extreme values of ν_d corresponded to samples from the same location in a coal mine ($19D5_H$ and $20D5_V$). In this case, the waves propagated faster through a vertical sample likely due to the slightly increased mineral content and less developed natural fracture network.

4.3. RELATIONSHIP OF MACERAL COMPOSITION, WAVE VELOCITIES AND DYNAMIC ELASTIC MODULI

Looking at the dependencies in Figure 5, a downward trend in the P- and S-wave velocities with a decrease in the mineral content in the samples are visible. Elevated wave velocities in samples of high mineral content ($4B_V$, $5B_V$, and $8B_H$) resulted in exceeding the E_d to ν_d limits for coal as proposed by Wu et al. (2019)—shown in the black rectangle in Figure 6.

Figure 7 shows the relationship between the *BI* and the mineral content in the samples. Samples from the B coal mine, of high mineral content, were characterized by an elevated *BI*. The only exception could be sample $8B_H$, of low mineral content, but relatively high *BI*. Low porosity (2.7 %) and an undeveloped developed fracture network resulted in greater consolidation in this case. The low mineral content in MS samples did not affect the *BI*.

In Figure 8 a trend of the maceral group content in the measured *BI* background can be seen. Samples containing more than 10 % mineral additives were not included in this comparison. There was a downward trend in the liptinite and inertinite content and an upward trend in the vitrinite content, with the decrease of *BI*. However, due to the small number of samples and significant differences in the composition of single samples, further research should be conducted to confirm or deny these trends.

5. CONCLUSIONS

The maceral composition analysis and laboratory ultrasonic measurements of coal core samples from the Upper Silesian Coal Basin (USCB) allow the following conclusions:

- A set of tested coal samples can be divided based on maceral content, into several groups: banded bright coals (containing mostly vitrinite), banded coals (where vitrinite and others maceral content are comparable) and banded dull coals (where vitrinite content is minor).
- The measured samples are characterized by velocities in the range of 1883-2700 m/s for P- and 990-1438 m/s for S-waves. Velocities are comparable to the literature data, however it should be noted that the values shown in literature are related to the coal samples of varied rank, composition and measured in specific conditions. Obtained dynamic elastic moduli: Young's (E_d) and Poisson's (ν_d) amounted to about 3.5-10.4 GPa, and 0.24-0.36 [-] respectively.
- The coal samples characterized by increased content of the mineral matter, reveal elevated velocities (about 2824-2989 m/s for P- and 1650-1700 m/s for S waves) and elastic moduli (about 10.9-13.2 GPa and in E_d and ν_d respectively). These values allow to easy distinguish between pure coal and mixed coal-mineral material.
- The brittleness indexes (*BI*) of measured samples, varied in the range of 39-91 %, reflect a good hydraulic fracturing potential. Significant amount of mineral matter in a few samples causes elevated E_d moduli and exceeding proposed *BI* limits for coal.
- A downward trend in the liptinite and inertinite content and an upward trend in the vitrinite content, with a decrease in the *BI,* were observed; however, due to the small number of samples, further research should be conducted to fully confirm these trends.

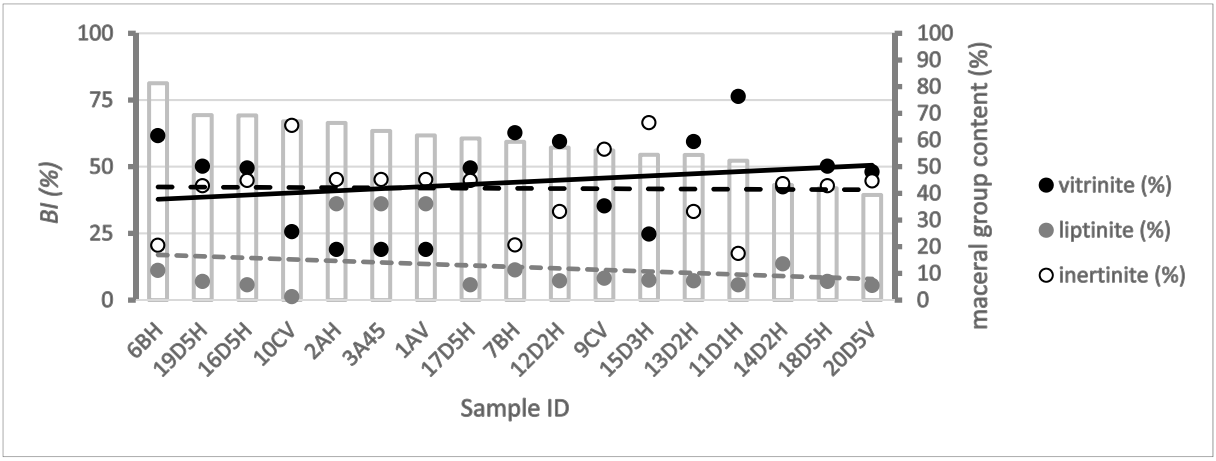

Fig. 8 Relationship between the BI and maceral composition in the measured samples. Black solid line: trend line (vitrinite), light grey dashed line: trendline (liptinite), and black dashed line: trend line (inertinite).

NOMENCLATURE

CBM	Coal bed methane,
BI	Brittleness index (%),
USCB	Upper Silesian Coal Basin, Poland,
ICCP	International Committee for Coal and Organic Petrology,
P	Bulk density (g/cm^3),
V_P	P-wave velocity,
V_S	S-wave velocity,
v_d	Dynamic Poisson's ratio (-),
E_d	Dynamic Youngs modulus (GPa),
G_d	Dynamic shear modulus (GPa),
K_d	Dynamic bulk modulus (GPa).

ACKNOWLEDGEMENT

This paper was made possible thanks to subsidies from the Ministry of Science and Higher Education of Poland for research activities, 2019–2020.

REFERENCES

Alramahi, B. and Sundberg, M.I.: 2012, Proppant embedment and conductivity of hydraulic fractures in shales. 46th U.S. Rock Mechanics/Geomechanics Symposium. ARMA, 12–291, 1–6. DOI: 10.2118/191124-PA

Altindag, R.: 2002, The evaluation of rock brittleness concept on rotary blast hole drills. J. South Afr. Inst. Min. Metall., 102, 1, 61–66.

Bała, M.: 1990, Classification of the sedimentary rocks based on the elastic moduli determined from the waveforms. Przegląd Geologiczny, 12, 556–559, (in Polish, with English summary).

Bała, M.: 2017, Characteristics of elastic parameters determined on the basis of well logging measurements and theoretical modeling, in selected formations in boreholes in the Baltic Basin and the Baltic offshore. Nafta-Gaz, 8, 558-570, (in Polish, with English abstract). DOI: 10.18668/NG.2017.08.03

Bishop, A.: 1967, Progressive failure with special reference to the mechanism causing it. Proceedings of the Geotechnical Conference on Shear Strength Properties of Natural Soils and Rocks. Oslo, Norway, 1967, 142–150.

Czupski, M., Kasza, P. and Wilk, K.: 2013, Fluids for fracturing unconventional deposits. Nafta-Gaz, 69, 42–50, (in Polish).

Diessel, C.: 1965, Correlation of macro and micropetrography of some New South Wales Coals. 8th Commonwealth Mining Metallurgical Congress, 6, Melbourne, 669–677.

Diessel, C.: 1992, Coal-bearing depositional systems. Springer-Verlag, Berlin. DOI: 10.1007/978-3-642-75668-9

Economides, M. and Martin, T.: 2007, Modern fracturing. Enhancing Natural Gas Production. ET Publishing, Houston, TX.

Garcia-Gonzalez, M. and Towle, G.: 2006, Measurements of elastic wave velocities in coal samples of differential rank. Boletin de Geol., 28, 1, 81–95.

Gonet, A., Nagy, S., Rybicki, C., Siemek, J., Stryczek, S. and Wiśniowski, R.: 2010, Technology of coal bed methane (CBM) extraction. Górnictwo i Geologia, 5, 3, 5–25, (in Polish, with English abstract).

Grieser, B. and Bray, J.: 2007, Identification of production potential in unconventional reservoirs. SPE Production and Operations Symposium, 31 March - 3 April 2007, Oklahoma City, USA. SPE 106623. DOI: 10.2118/106623-MS

Hajiabdolmajid, V. and Kaiser, P.: 2003, Brittleness of rock and stability assessment in hard rock tunneling. Tunn. Undergr. Space Technol., 18, 1, 35–48. DOI: 10.1016/S0886-7798(02)00100-1

Hucka, V. and Das, B.: 1974, Brittleness determination of rock by different methods. Int. J. Rock Mech. Min. Sci. Geomech. Abstr., 11, 10, 389–392. DOI: 10.1016/0148-9062(74)91109-7

International Committee for Coal and Organic Petrology (ICCP): 1998, The new vitrinite classification (ICCP System 1994). Fuel, 77, 5, 349–358. DOI: 10.1016/S0016-2361(98)80024-0

International Committee for Coal and Organic Petrology (ICCP): 2001, The new inertinite classification (ICCP System 1994). Fuel, 80, 4, 459–471. DOI: 10.1016/S0016-2361(00)00102-2

Jarvie, D., Hill, R., Ruble, T. and Pollastro, R.: 2007, Unconventional shale-gas systems: The Mississippian Barnett Shale of north-central Texas as one model for thermogenic shale-gas assessment. AAPG Bull., 91, 4, 475–499. DOI: 10.1306/12190606068

Jin, X., Shah, S., Roegiers, J.C. and Zhang, B.: 2014, Fracability evaluation in shale reservoirs – an integrated petrophysics and geomechanics approach. SPE Hydraulic Fracturing Technology Conference, 4-6 February 2014, The Woodlands, Texas, USA, 1–14, SPE 168589. DOI: 10.2118/168589-MS

Jin, X., Shah, S., Truax, J. and Roegiers, J.C.: 2014, A practical petrophysical approach for brittleness prediction from porosity and sonic logging in shale reservoirs. SPE Annual Technical Conference and Exhibition, 27-29 October 2014, Amsterdam, Netherlands, 1–21, SPE 170972. DOI: 10.2118/170972-MS

Jizba, D.: 1991, Mechanical and acoustical properties of sandstones and shales. Ph.D dissertation, Stanford University.

Kasza, P.: 2019, Hydraulic fracturing in unconventional reservoirs and methods of their analysis. Prace INiG-PIB, 226, (in Polish with English abstract). DOI: 10.18668/PN2019.226

Kumar, H., Mishra, S. and Mishra, M.: 2015, Experimental evaluation of geo mechanical properties of coal using sonic velocity. Advances in Agricultural, Biological & Environmental Sciences, 22-23 July 2015, London, UK. DOI: 10.15242/IICBE.C0715073

Li, Q., Chen, J. and He, J.: 2016, Laboratory measurements of the acoustic velocities and elastic property of coal rocks and their micro-features. SEG International Exposition and Annual Meeting, 16-21 October 2016, Dallas, US. DOI: 10.1190/segam2016-13877215.1

Luan, X., Di, B., Wei, J., Li, X., Qian, K., Xie, J. and Ding, P.: 2014, Laboratory measurements of brittleness anisotropy in synthetic shale with different cementation. SEG Technical Program Expanded Abstracts, 26-31 October 2014, Denver, USA, 3005–3009. DOI: 10.1190/segam2014-0432.1

Malon, A. and Tymiński, M.: 2019, Coal Bed Methane (CBM). In: Szuflicki, M., Malon, A. and Tymiński, M. (Eds.): A balance list of mineral resources in Poland as of the 31th December 2018. Polish Geological Institute-National Research Institute, Poland, (in Polish).

Masłowski, M., Kasza, P., Czupski, M., Wilk, K. and Moska, R.: 2019, Studies of fracture damage caused by the proppant embedment phenomenon in shale rock. Appl. Sci., 9, 11, 2190. DOI: 10.3390/app9112190

Morcote, A., Mavko, G. and Prasad, M.: 2010, Dynamic elastic properties of coal. Geophysics, 75, 6, E227–E234. DOI: 10.1190/1.3508874

Moska, R., Kasza, P. and Masłowski, M.: 2018, Rock anisotropy and brittleness from laboratory ultrasonic measurements in the service of hydraulic fracturing. Acta Geodyn. Geomater., 15, 1, 67–76. DOI: 10.13168/AGG.2018.0005

Moska, R. and Masłowski, M.: 2019, Attempts to determine the geomechanical and Thomsen's parameters of coal from Upper Silesian Coal Basin. Nafta-Gaz, 11, 700–707, (in Polish, with English abstract). DOI: 10.18668/NG.2019.11.05

Pickel, W., Kus J., Flores, D., Kalaitzidis, K., Christanis, K., Cardott, B.J., Misz-Kennan, M., Rodriges, S., Hentschel, A., Hamor-Vido, M., Crosdale, P. and Wagner, N.: 2017, Classification of liptinite-ICCP System 1994. Int. J. Coal Geol., 169, 40–61. DOI: 10.1016/j.coal.2016.11.004

Qian, K., Liu, T., Liu, J., Liu, X., He, Z. and Jiang, D.: 2020, Construction of a novel brittleness index equation and analysis of anisotropic brittleness characteristics for unconventional shale formations. Petroleum Science, 17, 70–85. DOI: 10.1007/s12182-019-00372-6

Qiuliang, Y. and De-hua, Han: 2008, Acoustic properties of coal from lab measurements. SEG Technical Program Expanded Abstracts, 27, No. 1. DOI: 10.1190/1.3059254

Rickman, R., Mullen, M., Petre, E., Grieser, B. and Kundert. A.: 2008, A practical use of shale petrophysics for stimulation design optimization: All shale plays are not clones of the Barnett Shale. SPE Annual Technical Conference and Exhibition, 21-24 September 2008, Denver, Colorado, USA, SPE115258. DOI: 10.2118/115258-MS

Sykorova, J., Pickel, W., Christianis, K., Wolf, M., Taylor, G. and Flores, D.: 2005, Classification of huminte - ICCP System 1994. International Journal of Coal Geology, 62, No. 1-2, 85–106. DOI: 10/1016/j.coal.2004.06.006

Tarasov, B. and Potvin, Y.: 2013, Universal criteria for rock brittleness estimation under triaxial compression. International Journal of Rock Mechanics and Mining Sciences, 59, 57–69. DOI: 10.1016/j.ijrmms.2012.12.011

Vernik, L.: 1993, Microcrack-inducted versus intrinsic elastic anisotropy in mature HC – source shales. Geophysics, 58, No. 11, 1703–1706. DOI: 10.1190/1.1443385

Wang, F. and Gale, J.: 2009, Screening Criteria for Shale-Gas Systems. Gulf Coast Association of Geological Societes Transactions, 59, 779–793.

Wu, H., Dong, S., Li, D., Huang, Y. and Qi, X.: 2015, Experimental study on dynamic elastic parameters of coal samples. International Journal of Mining Science and Technology, 25, 447–452. DOI: 10.1016/j.ijmst.2015.03.019

Wu, H., Zhang, P., Dong, S., Huang, Y. and Zhang, M.: 2019, Brittleness index analysis of coal samples. Acta Geophysica, 67, 789–797. DOI: 10.1007/s11600-019-00291-5

Yu, G., Vozoff, K. and Durney, D.W.: 1993, The influence of confining pressure and water saturation on dynamic elastic properties of some Permian coals. Geophysics, 58, No. 1, 30–38. DOI: 10.1190/1.1443349

Zhang, D., Ranjith, P. and Perera, M.: 2016, The brittleness indices in rock mechanics and their application in shale hydraulic fracturing: A review. Journal of Petroleum Science and Engineering, 143, 158–170. DOI: 10.1016/j.petrol.2016.02.011

Attachment 1 Comparison of selected elastic parameters of the measured coal samples and from the literature data.

	This paper				Qiuliang and De-hua (2008)	Morcote et al. (2010)	Wu et al. (2015)	Li et al. (2016)	Wu et al. (2019)
Measurement conditions	*T* of about 25 °C, conf. *p* at 9.72 MPa				variable diff. *p*	conf. *p* at 10.0 MPa	conf. *p* at 10.0 MPa	conf. *p* at 10.0 MPa	NPT *T* of about 25°C, 1 bar *p*
Coal type	banded dull coal, dry	banded bright coal, bright coal, water saturated	banded dull coal, water saturated	mostly banded coal, water saturated	coal, silty coal, shaly coal, dry and water saturated	bituminous coal, dry	anthracite coal, dry	mostly vitrinite with inertinite and calcite additive, dry	anthracite coal, dry
ρ (g/cm^3)	1.27–1.28	1.38–1.95	1.35–1.41	1.31–1.39	1.36–1.73	1.30–1.34	1.45–1.61	-	1.378–1.485
V_p (m/s)	2378–2430	2293–2989	1969–2131	1883–2296	2320–2560	about 2100–2600	2220–2632	2260–2540	1307–2602
V_s (m/s)	1261–1328	1207–1700	1076–1202	990–1172	1080–1250	about 950–1200	1091–1382	1060–1150	452–1388
v (-)	0.29–0.30	0.24–0.31	0.27–0.29	0.24–0.36	-	-	0.27–0.35	-	0.24–0.46
E (GPa)	5.32–5.77	5.27–13.18	4.01–5.16	3.58–4.78	-	-	4.62–8.05	3.70–4.30	0.846–7.331
BI (%)	61.69–66.42	59.31–>100*	56.06–67.00	39.42–69.36	-	-	-	-	3.10–77.42

* *BI* over 100 % results from increased content of the mineral matter in the coal samples.